Two-step-only phase-shifting interferometry with optimized detector bandwidth for microscopy of live cells

Natan T. Shaked*, Yizheng Zhu, Matthew T. Rinehart, and Adam Wax

Department of Biomedical Engineering, Fitzpatrick Institute for Photonics, Duke University
Durham, North Carolina 27708, USA.
**natan.shaked@duke.edu*

Abstract: We present a phase-shifting interferometric technique for imaging live biological cells in growth media, while optimizing spatial resolution and enabling potential real-time measurement capabilities. The technique uses slightly-off-axis interferometry which requires less detector bandwidth than traditional off-axis interferometry and fewer measurements than traditional on-axis interferometry. Experimental and theoretical comparisons between the proposed method and these traditional interferometric approaches are given. The method is experimentally demonstrated via phase microcopy of live human skin cancer cells.

OCIS codes: (170.3880) Medical and biological imaging; (180.3170) Interference microscopy; (090.2880) holographic interferometry; (090.1995) Digital holography.

References and links

1. P. Marquet, B. Rappaz, P. J. Magistretti, E. Cuche, Y. Emery, T. Colomb, and C. Depeursinge, "Digital holographic microscopy: a noninvasive contrast imaging technique allowing quantitative visualization of living cells with subwavelength axial accuracy," Opt. Lett. **30**(5), 468–470 (2005).
2. T. Ikeda, G. Popescu, R. R. Dasari, and M. S. Feld, "Hilbert phase microscopy for investigating fast dynamics in transparent systems," Opt. Lett. **30**(10), 1165–1167 (2005).
3. E. Cuche, P. Marquet, and C. Depeursinge, "Spatial filtering for zero-order and twin-image elimination in digital off-axis holography," Appl. Opt. **39**(23), 4070–4075 (2000).
4. I. Yamaguchi, and T. Zhang, "Phase-shifting digital holography," Opt. Lett. **22**(16), 1268–1270 (1997).
5. C. P. Brophy, "Effect of intensity error correlation on the computed phase of phase-shifting interferometry," J. Opt. Soc. Am. A **7**(4), 537–541 (1990).
6. Y. Awatsuji, M. Sasada, and T. Kubota, "Parallel quasi-phase-shifting digital holography," Appl. Phys. Lett. **85**(6), 1069–1071 (2004).
7. N. T. Shaked, M. T. Rinehart, and A. Wax, "Dual-interference-channel quantitative-phase microscopy of live cell dynamics," Opt. Lett. **34**(6), 767–769 (2009).
8. X. F. Meng, L. Z. Cai, X. F. Xu, X. L. Yang, X. X. Shen, G. Y. Dong, and Y. R. Wang, "Two-step phase-shifting interferometry and its application in image encryption," Opt. Lett. **31**(10), 1414–1416 (2006).
9. J. P. Liu, and T. C. Poon, "Two-step-only quadrature phase-shifting digital holography," Opt. Lett. **34**(3), 250–252 (2009).
10. G. L. Chen, C. Y. Lin, H. F. Yau, M. K. Kuo, and C. C. Chang, "Wave-front reconstruction without twin-image blurring by two arbitrary step digital holograms," Opt. Express **15**(18), 11601–11607 (2007).
11. T. M. Kreis and W. P. P. Jupiter, "Suppression of the dc term in digital holography," Opt. Eng. **36**(8), 2357–2360 (1997).
12. Y. Takaki, H. Kawai, and H. Ohzu, "Hybrid holographic microscopy free of conjugate and zero-order images," Appl. Opt. **38**(23), 4990–4996 (1999).
13. Y. Zhang, Q. Lu, and B. Ge, "Elimination of zero-order diffraction in digital off-axis holography," Opt. Commun. **240**(4-6), 261–267 (2004).
14. E. Tajahuerce, O. Matoba, S. C. Verrall, and B. Javidi, "Optoelectronic information encryption with phase-shifting interferometry," Appl. Opt. **39**(14), 2313–2320 (2000).
15. K. J. Chalut, W. J. Brown, and A. Wax, "Quantitative phase microscopy with asynchronous digital holography," Opt. Express **15**(6), 3047–3052 (2007).
16. J. Schmit, and K. Creath, "Extended averaging technique for derivation of error-compensating algorithms in phase-shifting interferometry," Appl. Opt. **34**(19), 3610–3619 (1995).

#111913 - $15.00 USD Received 26 May 2009; revised 30 Jul 2009; accepted 11 Aug 2009; published 19 Aug 2009

1. Introduction

Interferometric phase microscopy of nearly-transparent live biological cells yields quantitative measurement of the associated optical path delays, and thus can be an important tool for medical diagnostics and cell biology studies [1,2]. However, these applications require special and careful considerations to minimize the effects of mechanical vibrations which can arise due to sample mounting and immersion in growth media. This vulnerability emphasizes the necessity for minimizing the number of camera exposures without sacrificing spatial frequency bandwidth which can limit detection of fine details.

Two general interferometric approaches are presented in the literature: off-axis interferometry and on-axis interferometry. Off-axis interferometry [3] is based on interfering off-axis beams, where the entire object wave front is recorded by a single digital camera exposure. This technique is suitable for the acquisition of dynamic processes such as live cells in growth media as the influence of mechanical vibrations is minimized by the use of a single exposure. However, this approach requires a spatial-frequency separation between the desired positive-order diffracted wave and the unwanted zero- and negative-order diffracted waves. Thus, the spatial frequency bandwidth of the reconstructed image is limited by the presence of these unwanted waves. Spatial filtering is traditionally used to separate the desired wave. However, the number and size of the digital camera pixels place limitations on the carrier frequency needed to create this separation and important information may be lost.

In on-axis interferometry [4], on the other hand, the angle between the reference and object beams is zero, yielding a narrower spatial frequency bandwidth of the interferometric signal. However, in this case, at least three phase-shifted interferograms are needed to separate the unwanted waves from the desired wave. It has been shown that the reconstruction errors increase as the number of interferograms increases, when acquired sequentially [5].

Simultaneous acquisition of several interferograms is proposed in Refs [6,7], which provides a suitable approach for visualizing dynamic processes. However, to avoid further reconstruction errors, equalization of intensity variations and accurate digital image registration must be performed when separating a single camera image into several different digital interferograms, and thus this approach might not be preferred for certain applications.

Meng *et al.* [8] have suggested a phase-shifting interferometric method in which only two on-axis interferograms and a separate reference wave intensity measurement are needed, under the condition that the intensity of the reference wave is large enough. In this method, the reference intensity distribution has to be re-measured if it changes during the interferometric recording. Liu and Poon [9] have recently suggested an improved method in which only two on-axis interferograms and an estimation (rather than a measurement) of the reference field are needed. A different estimation method has been suggested by Chen *et al.* [10]. These methods can reconstruct the object field with relatively small errors.

In the current paper, we suggest an alternative approach in which only two interferograms are needed. This method requires neither former knowledge nor prediction of any of the fields to recover phase information. Furthermore, it does not require a detector with as much spatial frequency bandwidth as that needed for traditional off-axis interferometry. The proposed method provides an intermediate solution between on-axis and off-axis interferometry. In the proposed method, the sample phase is obtained by using only two slightly-off-axis phase-shifted interferograms, without offline measurements or estimations, and a simple digital process that can be implemented in real time. Spatial frequency considerations in digital interferometry are well documented in the literature (e.g [3].). In addition, different methods have been suggested to suppress the dc term in traditional off-axis interferometry [11–13]. However, to the best of our knowledge, the method proposed in this paper has not been suggested as a means to optimize the tradeoff between the acquisition rate and the detector bandwidth for quantitative phase microscopy of live biological cells in growth media.

#111913 - $15.00 USD Received 26 May 2009; revised 30 Jul 2009; accepted 11 Aug 2009; published 19 Aug 2009

2. Slightly-off-axis interferometry principle

Figure 1 illustrates an interferometric setup for sequentially acquiring two or more phase-shifted interferograms. Linearly-polarized light from a coherent laser source is split into reference and sample beams using a modified Mach Zehnder interferometer. To preserve the phase and amplitude information, lenses L_1 and L_3, as well as lenses L_2 and L_3, are positioned in 4f configurations. By varying their orientations, the two wave plates positioned in the reference arm can create different phase shifts between the interferograms generated on the camera. This simple setup is based on the phase-shifting method proposed in Ref [14], but has been adapted for microscopy. Other phase-shifting configurations, such as the ones presented in Refs [7] and [15], are also possible for implementing the proposed method.

According to the slightly-off-axis interferometric approach, only two slightly-off-axis interferograms $I_k, k = 1,2$ are acquired. These interferograms can be expressed as follows:

$$I_k = |E_r|^2 + |E_s|^2 + |E_s||E_r^*|\exp[j(\varphi_{OBJ} + qx + \alpha_k)] + |E_r||E_s^*|\exp[-j(\varphi_{OBJ} + qx + \alpha_k)], \quad (1)$$

where E_r and E_s are respectively the reference and sample field distributions, φ_{OBJ} is the spatially-varying phase associated with the object, q is the fringe frequency due to the angular shift between the sample and reference fields, and $\alpha_1 = 0$, $\alpha_2 = \beta$ define the phase shift induced between the interferograms by the wave plates. From Eq. (1), it can be seen that incorrect estimation of β or q will add constant or modulated phase errors to the calculated object phase. Therefore, although q and β can be measured or calculated in advance, these parameters are digitally measured after each frame of acquisition, providing an advantage in canceling variations in these parameters introduced during multiple measurements. Assuming a horizontal fringe pattern, these parameters can be calculated by summing the fringe pattern columns and fitting the resulting vector to a sine wave. This process allows us to find q and β with high enough accuracy to prevent degradation of the phase modulation induced by the object. Once the two interferograms have been acquired, they can be digitally processed to recover the recorded sample's wrapped phase distribution as follows:

$$F = \left[I_1 - I_2 + j \cdot \mathrm{HT}\ \ I_1 - I_2 \ \right] \cdot \exp(-jqx) \Big/ 1 - \exp(j\beta)\ , \varphi_{OBJ} = \arctan\ \ \mathrm{Im}\,F / \mathrm{Re}\,F\ \ , (2)$$

where HT denotes a Hilbert transform. The spatial frequency representation of each of the interferograms includes two autocorrelation terms (ACTs), both located at the origin of the spatial frequency domain, and two crosscorrelation terms (CCTs), each located on a different side of the spatial frequency domain. Assuming that the CCTs are spatially separated, Eq. (2) demonstrates mathematically how to isolate the positive-frequency CCT from both ACTs and the negative-frequency CCT, and then center the positive-frequency CCT at the origin of the

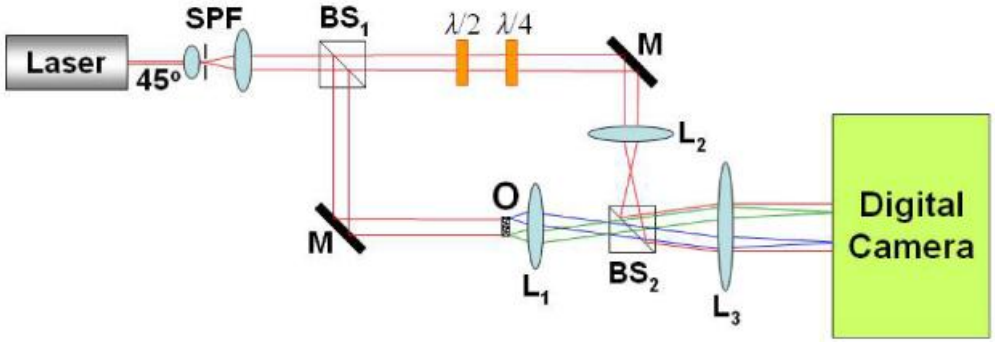

Fig. 1. Possible experimental setup for phase-shifting interferometry. SPF = Spatial filter (beam expander with a confocally-positioned pinhole), BS_1, BS_2 = Beam splitters; M = Mirror; λ/2 = Half wave plate; λ/4 = Quarter wave plate; O = Object/Sample; L_1, L_2, L_3 = Lenses.

#111913 - $15.00 USD Received 26 May 2009; revised 30 Jul 2009; accepted 11 Aug 2009; published 19 Aug 2009

spatial-frequenacy domain by a multiplication with $\exp(-jqx)$. The arctan function in Eq. (2) yields the wrapped phase profile of the object, and an unwrapping algorithm is then used to remove 2π phase ambiguities in the phase profile.

3. Slightly-off-axis versus traditional off-axis and on-axis interferometry

To illustrate the advantage of the proposed approach, we theoretically compare the spatial frequency spectra of three methods: traditional off-axis, slightly-off-axis, and traditional on-axis interferometry. These spectra are illustrated in Fig. 2, where for simplicity only one spatial frequency axis is shown. In all cases the ACTs, located around the origin of the spatial spectrum, are composed of the reference-field and sample-field ACTs. Since the reference field is assumed to be a constant plane wave over the camera illumination area, the total width of the ACTs for an image interferogram is solely dominated by the width of the sample-field ACT given by four times the highest spatial frequency ω_0 of the object imaged on the camera. In comparison, the width of each CCT is only $2\omega_0$. As shown in Fig. 2(a), traditional off-axis interferometry requires that the angle between the reference and object beams completely separates the CCTs from the ACTs. This occurs when $q \geq 3\omega_0$, resulting in a highest spatial frequency of at least $4\omega_0$. Note that ω_0 can be experimentally measured once before the object real-time acquisition, under the reasonable assumption that it stays constant during the multiple measurements of the object. Alternatively, for biological cell microscopy, ω_0 is usually inversely proportional to the diffraction-limited spot of the optics.

For slightly-off-axis interferometry, the CCTs should not overlap, but overlap of the ACTs with each of the CCTs is allowed. As shown in Fig. 2(b), this occurs for $q = \omega_0$. Therefore, the highest spatial frequency needed per exposure is only $2\omega_0$, half of that needed in the traditional off-axis interferometry. Thus, when the maximum fringe frequency allowed by the camera does not create enough separation between the ACTs and the CCTs, an advantage can be gained by acquiring two off-axis interferograms and process them using the slightly-off-axis interferometric technique described by Eq. (2), instead of acquiring a single off-axis interferogram. This will be demonstrated experimentally in the next section.

In the case of on-axis interferometry, shown in Fig. 2(c), all CCTs and ACTs are centered at the origin. Therefore, the necessary highest spatial frequency per exposure is only ω_0. However, in this case three or four interferograms (depending on the technique chosen) must be acquired to fully eliminate both ACTs and one of the CCTs.

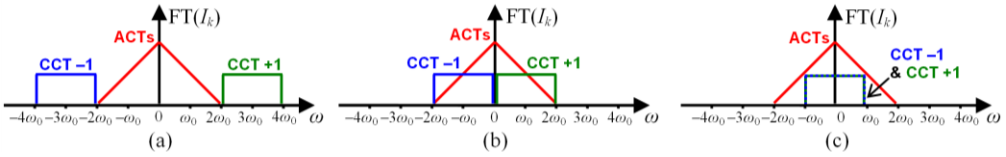

Fig. 2. Schematic comparison between the spatial-frequency domains of (a) off-axis interferometry, (b) slightly-off-axis interferometry, and (c) on-axis interferometry. For simplicity, only one spatial-frequency axis is shown.

For observing dynamic processes, it is better to acquire the data with as few measurements as possible to minimize reconstruction errors and data acquisition times. In this aspect, slightly-off-axis interferometry is superior to on-axis interferometry. In addition, traditional on-axis interferometry requires strict control of the phase shifts between the interferograms since even slight variations can introduce reconstruction errors [16]. The proposed slightly-off-axis method avoids this type of errors by digitally measuring the exact phase shift between the interferograms after the acquisition of each sample instance. To find the exact phase shifts for on-axis interferometry, fitting to a Fresnel zone plate is possible, but then detector space is scarified for displaying the high-order rings of the Fresnel zone plate pattern.

#111913 - $15.00 USD Received 26 May 2009; revised 30 Jul 2009; accepted 11 Aug 2009; published 19 Aug 2009

4. Experimental results

To experimentally demonstrate the proposed method, the optical system shown in Fig. 1 was used. Linearly-polarized light from a 17 mW HeNe laser was split by the modified Mach-Zehnder interferometer. Two 40× microscope objectives were used as L_1 and L_2, while L_3 was a simple spherical lens with a focal length of 15 cm, creating a magnification of 33× on the CCD sensor plane (AVT Pike F032-B, 640×480, 7.4μm×7.4μm pixels). For the experiments, a restricted region of 120×120 pixels was used, with the fringe frequency set to 15 or 18 cycles/mm, depending on the experiment set. These reduced frequencies were chosen for the clarity of each demonstration.

In the first set of experiments, a static water-immersed polystyrene microsphere (Duke Scientific Corporation, 12μm diameter) on a microscope coverslip was used as the object. Figure 3(a) demonstrates the low visibility of a simple intensity image of the sample. Phase reconstructions using off-axis, slightly-off-axis, and on-axis geometries were executed. For the off-axis case, the best spatial resolution can be achieved when the fringe frequency on the camera is set to the maximum fringe frequency allowed in this demonstration (restricted to 15 cycles/mm as stated above) with the resulting interferogram shown in Fig. 3(b). However, as shown in the spatial-frequency domain of the interferogram [Fig. 3(c)], this fringe frequency was not high enough to separate the ACTs and CCTs. Figure 3(d) shows the corresponding reconstructed wrapped phase, and Figs. 3(e) and (f) show the final unwrapped phase, demonstrating the low quality obtained by traditional off-axis interferometry under these restrictions. To demonstrate the utility of slightly-off-axis interferometry, another interferogram was acquired with the same fringe frequency but with a 90° phase shift introduced by a 90° rotation of the quarter wave-plate (see Fig. 1). The two interferograms were processed according to Eq. (2), yielding the wrapped phase shown in Fig. 3(g) and the unwrapped phase shown in Figs. 3 (h) and (i), demonstrating the improvement that was obtained by the slightly-off-axis technique. For comparison, four on-axis interferograms (with phase shifts of 0°, 90°, 180°, and 270°) were obtained by varying the relative orientations of the half wave plate and the quarter wave plate [14], with the reconstructed wrapped phase shown in Fig. 3(j) and the corresponding unwrapped phase shown in Figs. 3 (k) and (l). From the smoothness of the shape and the flatness of the background, the traditional on-axis technique performed comparably to the slightly-off-axis technique although it required twice as many images. To quantify these results, fitting Figs. 3 (f), (i), and (l) to a simulated phase projection of the microsphere with a flat background yielded root-squared-value accuracies of 91% for off-axis, 98% for slightly-off-axis, and 99% for on-axis, respectively.

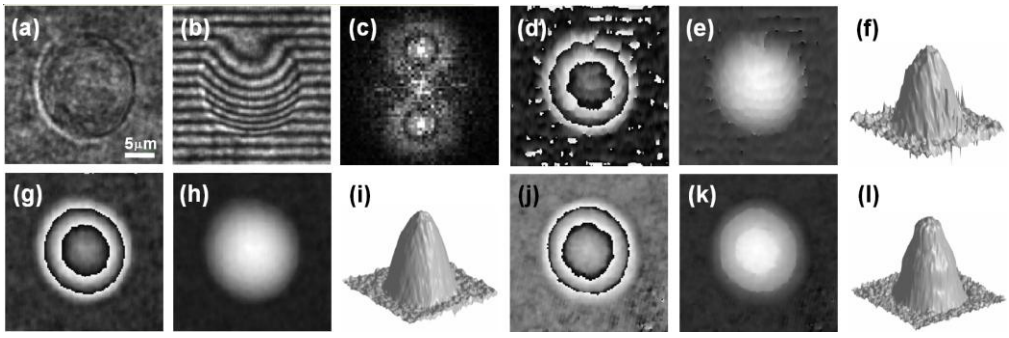

Fig. 3. Static polymer microsphere (12μm in diameter): (a) Regular intensity image through the system; (b) Single off-axis interferogram; (c) The middle part of the spatial spectrum of the interferogram shown in (b). Digitally reconstructed phase obtained by: (d-f) traditional off-axis interferometry (using a single interferogram), (g-i) slightly-off-axis interferometry (using two phase-shifted interferograms), (j-l) on-axis interferometry (using four phase-shifted interferograms). (d,g,j) Wrapped phases; (e,h,k) Final unwrapped phases; (f,i,l) Surface plots of the final unwrapped phases shown in (e,h,k), respectively.

#111913 - $15.00 USD Received 26 May 2009; revised 30 Jul 2009; accepted 11 Aug 2009; published 19 Aug 2009

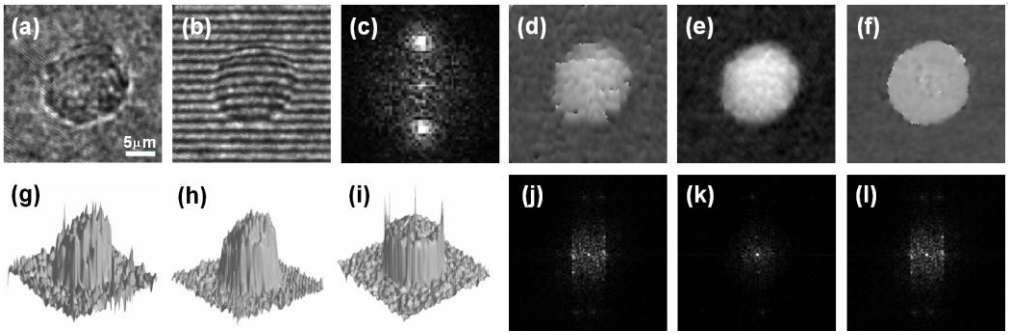

Fig. 4. Live human skin cancer (A431, epithelial carcinoma) cell in growth media: (a) Regular intensity image through the system; (b) Single off-axis interferogram; (c) The middle part of the spatial spectrum of the interferogram shown in (b); (d-f) Final unwrapped phase obtained by: (d) traditional off-axis interferometry (using a single interferogram), (e) slightly-off-axis interferometry (using two phase-shifted interferograms), (f) on-axis interferometry (using four phase-shifted interferograms); (g-i) Surface plots of the final unwrapped phases shown in (d-f), respectively; (j-l) MTF images of the background of (d-f), respectively.

In the second set of experiments, we visualized a human skin cancer cell (A431, epithelial carcinoma) in growth media. The direct image of this sample through the system is shown in Fig. 4(a). A single off-axis interferogram of the sample and its spatial frequency domain representation are shown in Figs. 4(b) and (c), respectively, where again there was not enough separation between the ACTs and CCTs, and thus the final unwrapped phase [Figs. 4(d,g)] is highly degraded. For the slightly-off-axis interferometry case, an additional 90° phase-shifted interferogram of the same sample was acquired. Both interferograms were processed according to Eq. (2) and an unwrapping algorithm was applied to the result yielding the final unwrapped phase shown in Figs. 4(e,h). Again, from the flatness of the background and the texture of the cell, it can be seen that substantial improvement is obtained by the slightly-off-axis interferometric approach compared to the traditional off-axis approach.

For comparison, four on-axis interferograms, each phase-shifted by 90°, were acquired for the same sample. However, for cancer cells in growth media, the final unwrapped phase for the on-axis case [Figs. 4(f,i)] was worse compared to the slightly-off-axis case [Figs. 4(e,h)], especially at the cell boundaries. One cause for the degraded image in Figs. 4(f,i) was the vibrations and Brownian motion of the cell media. Consequently, it was much harder to obtain the accurate phase shifts required in the traditional on-axis case. On the other hand, for the slightly-off-axis case, the exact phase shifts were easily found by digitally fitting the background fringes to sine waves, and thus temporal phase-shift errors were avoided. In addition, slightly-off-axis interferometry required only two measurements, rather than four, which made the phase profile less sensitive to sample changes due to motion between the measurements and resulted in a higher image throughput. To quantify the improvement of the proposed method for the cell measurement as well, Figs. 4 (j-l) show the modulation transfer function (MTF) of the image background (growth media with no cell present) of Figs. 4(d-f), respectively. Excluding the dc point at the center, the half-power-bandwidth in the vertical dimension for the slightly-off-axis case is 0.31 and 0.34 of the two other cases. The fact that the slightly-off-axis MTF [Fig. 4(k)] is narrower than in the two other cases [Figs. 4(j) and (l)] indicates a flatter background, and consequently smother overall phase profile for the slightly-off-axis case.

5. Conclusion

We have proposed a two-step-only phase-shifting interferometry scheme in which only two slightly-off-axis interferograms are needed, with no offline measurements or approximations of the sample or the reference fields required. The proposed method is an intermediate

#111913 - $15.00 USD Received 26 May 2009; revised 30 Jul 2009; accepted 11 Aug 2009; published 19 Aug 2009

solution between the well-known off-axis interferometric approach and the phase-shifting on-axis interferometric approach. We believe that the new approach will be useful as a powerful tool for interferometric phase measurements of dynamic processes with fine spatial details, especially for observing live biological cell dynamics.

Acknowledgements

We thank Dr. Daniel L. Marks for his advices and Matthew J. Crow for his help in preparing the cell samples. This work was supported by a grant from the National Science Foundation (NSF) (BES 03-48204). N.T.S. greatly acknowledges the support of the Bikura Postdoctoral Fellowship from Israel.

#111913 - $15.00 USD Received 26 May 2009; revised 30 Jul 2009; accepted 11 Aug 2009; published 19 Aug 2009